Interferences in AC–DC LED Drivers Exposed to Voltage Disturbances in the Frequency Range 2–150 kHz

Selcuk Sakar, *Student Member, IEEE*, Sarah Rönnberg, *Senior Member, IEEE*, and Math Bollen, *Fellow, IEEE*

***Abstract*—LED lamps are both potential victims and sources of electromagnetic disturbances in the frequency range between 2 and 150 kHz (“supraharmonics”). Immunity tests for this frequency range are important due to possible performance degradation of light intensity with LED lamps. In this paper, the impact of supraharmonics (SHs) on light intensity from LED lamps has been analyzed. LED lamps have been exposed to SH test profiles based on IEC 61000-4-19. Three phenomena that impact light intensity metrics have been observed and explained by models: 1) earlier conduction/later blocking caused by SH voltage, 2) intermittent conduction depending on the SH impedance of the LED driver, and 3) reverse-recovery current of the diodes at higher frequency. It is observed that impact on the light intensity metrics shows up around the beginning and end of the conduction period. The results reveal that the profile of the SH voltage could cause deviations in the modulation depth and the average light intensity. The immunity of LED lamps against SHs shall be further studied and discussed by research groups and standard committees.**

***Index Terms*—AC–DC power converters, electromagnetic compatibility, immunity testing, LED lamps, lighting, power quality, power-system harmonics, supraharmonics (SHs), switching converters.**

I. Introduction

INCREASING connection of power electronic-based equipment, such as electric vehicles and inverters, into the> grid has raised an issue of electromagnetic emission between 2 and 150 kHz also known as “supraharmonics” [1]–[3]. Supraharmonics (SHs) are injected by switching of power electronics-based equipment and by power line communication (PLC) systems, and can cause interference to devices connected nearby [3], [4]. Malfunction of electronic meters and household appliances, such as LED lamps, has been reported in both United States and Europe, especially when they are connected with photovoltaic inverters and other power electronic-based devices [5]–[7].

Manuscript received October 15, 2018; revised December 20, 2018; accepted February 5, 2019. Date of publication February 13, 2019; date of current version August 29, 2019. This work was supported by the project titled Light Intensity Variations of LED Lighting—Relation With Disturbances in the Voltage (P42468-1). Recommended for publication by Associate Editor M. Ponce-Silva. *(Corresponding author: Selcuk Sakar.)*

The authors are with the Electric Power Engineering, Luleå University of Technology, Skellefteå 931 87, Sweden (e-mail:

between LED lamps' current at the SH range has been studied by taking into account different driver topologies [23]. It was observed that resonance can be activated at different frequency ranges when connecting multiple LED lamps [23], [24].

The impact of SHs on light intensity from LED lamps has been studied by several papers. The work in [23] and [25] showed impact particularly around the zero crossing and peak of the grid voltage. Furthermore, it was shown that the impact of a SH pulse shorter than one cycle depends on where in the cycle the pulse occurs. Although those studies cover the application of SHs on LED lamps, it is limited by the application of discrete samples instead of sweeping the frequency. In [6], LED lamps were exposed to the test profiles defined in IEC 61000-4-19 [7]. It was shown that the non-synchronization between the grid and the SH test profiles could result in intermodulation of the light intensity variation.

Earlier studies only deal with the rectangular modulated (RM) test profile defined in IEC 61000-4-19 [6]. For a complete analysis, it is required to analyze the continuous wave (CW) test profile, too. In addition, none of the earlier studies paid any attention to the role of the LED drivers and factors behind the light intensity variations.

This paper describes the interaction between light intensity variations and SHs for LED lamps with respect to the CW SH test profile. Sixteen lamps and two evaluation boards have been exposed to voltage disturbances from 2 to 150 kHz. The measurements have been analyzed with respect to light intensity metrics such as modulation depth (MD) and average light intensity. It has been also analyzed how the position of SH test profiles within a cycle impacts the light intensity. Three phenomena, which can impact the light intensity metrics, have been observed due to SHs at the lamps' terminal. A model and reasoning have been constituted for verification of the experimental results

II. Method

This section describes the measurement setup and calculations performed for the study as follows.

A. Testing of LED Lamps

For the testing of the LED lamps, a number of lamps and evaluation boards have been obtained from different brands available on the market. Three examples, two LEDs and one evaluation board, are shown here to illustrate the phenomena, which can impact the light intensity metrics. The measurements are performed by using WW5064 arbitrary waveform generator and AE Techron 7224 amplifier to generate the signals. The light intensity signal is measured by Hagner S2 photometer that can measure up to 10 kS/s. The lamps are placed into an enclosure for proper and reliable data capture of the light intensity. Yokogawa DL850 oscilloscope that has a sampling rate of 10 MS/s is used for acquiring data. The setup for the measurements is shown in Fig. 1.

Two main sources of SHs in the grid are PLC systems and power electronic converter units. For representing such emissions, two test profiles are defined in IEC 61000-4-19:2012: a CW test profile and an RM test profile. The emissions due to power electronics and longer term PLC disturbances, which last more than 3 s, in the grid are represented by the CW test profile. The RM profile is representative of the non-intentional current or voltage from converters as well as intentional PLC signals. This study is limited to the CW test profile.

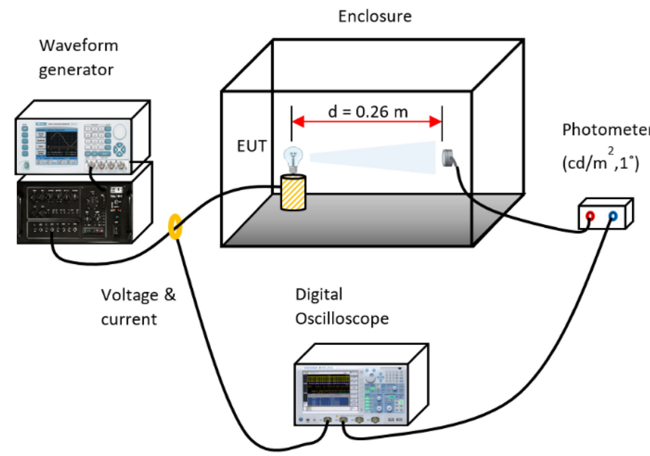

Fig. 1. Measurement setup.

The test of the CW profile is performed from 2 to 150 kHz applying 3 s pulses at corresponding SH, as given in Fig. 2(a), with 200 ms pause time. Superimposing of the CW profile on the supply voltage is carried out in MATLAB, synchronized at the zero crossing, and .wav files are generated to upload into arbitrary waveform generator. Amplified signal as 230 V–50 Hz including SH voltages is run at the lamp's terminal as given in Fig. 1.

The magnitude of the SH voltage can be chosen based on the description of the classified environment of the equipment, as shown in Fig. 2(b), based on IEC 61000-4-19:2012 [7]. In this study, to be able to study the impact of the SH voltage and frequency individually, it was decided to perform the test by sweeping the frequencies with a constant voltage as given in Fig. 2(b). The test was performed by increasing the voltage with 1 V for each iteration from 1 up to 12 V with respect to IEC 61000-4-19:2012 [7]. Each voltage is applied from 2 to 150 kHz in 45 steps.

B. Calculation of Metrics

For the interpretation of the light intensity signal, following metrics have been used.

1) Modulation Depth: MD is a measure of relative modulation amplitude or also known as peak to peak contrast [18]. The MD is influenced mainly by the component at twice the power system frequency (2 times 50 Hz in Sweden) showing up due to limitations in the ac–dc rectification. A light intensity variation at 100/120 Hz cannot be perceived by an average human observer but it is considered as a metric that shall be kept low as it can have adverse health effects [26]. Fig. 3 shows a representative light intensity signal and the parameters to calculate the

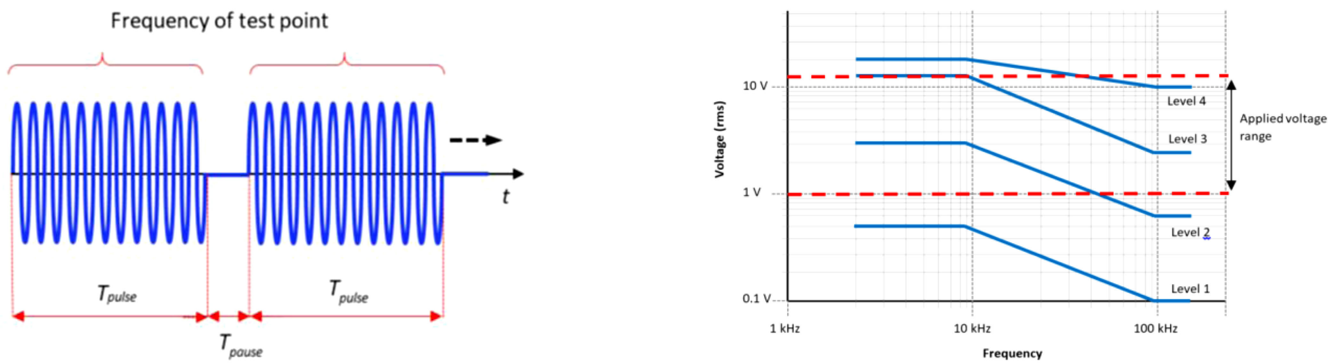

(a) (b)

Fig. 2. (a) CW test profile contains 3 s pulse and 200 ms pauses. (b) Test levels based on classified environment of equipment, Level 3 correspond to residential environment in [13].

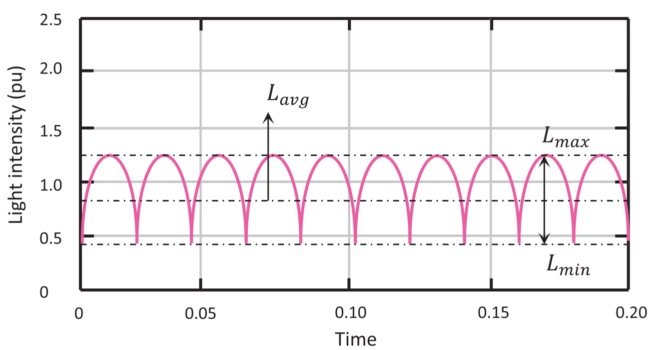

Fig. 3. Representative light intensity signal-full wave rectified.

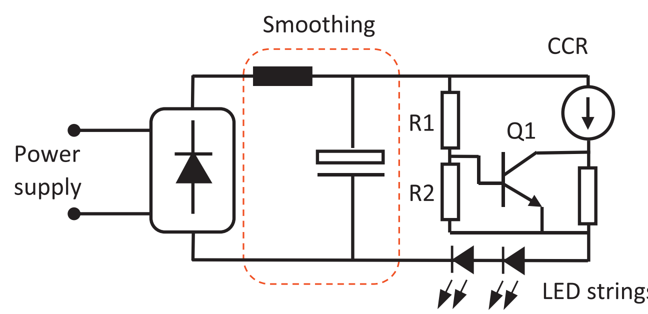

Fig. 4. Typical CCR (linear) LED driver circuit.

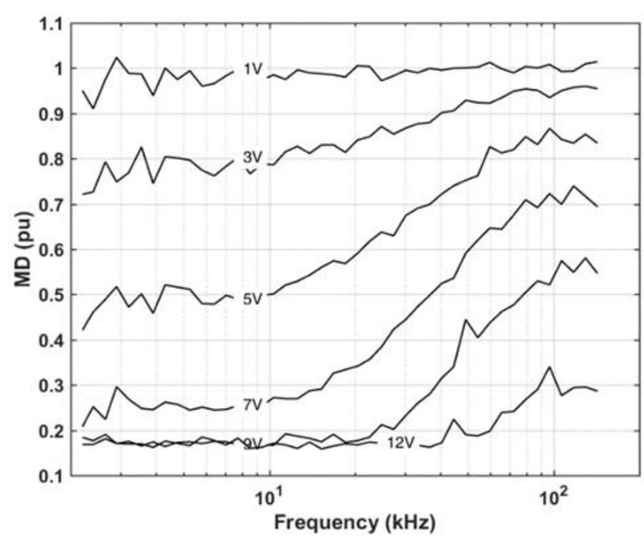

Fig. 5. LED 02 MD as a function of frequency for different supraharmonic voltages.

MD according to the following equation:

$$\mathrm{MD}\,(\%) = 100 \times \frac{(L_{\max} - L_{\min})}{(L_{\max} + L_{\min})} \tag{1}$$

where $L_{\max}$ and $L_{\min}$ are the maximum and minimum values of the light intensity signal within the observed period of the signal, respectively. All calculations performed in the following sections are performed based on (1).

2) Average Light Intensity: Averaging of instantaneous light intensity values during one period of 50 Hz indicates the strength of the light intensity signal. The average light intensity is employed as a metric for analyzing the impact of SHs on LED lamps. A representative light intensity signal showing average magnitude is shown in Fig. 3.

III. Observation and Analysis

In this section, experimental results of LED lamps exposed to SHs are presented and evaluated. All lamps have first been measured when supplied by the supply voltage (230 V, 50 Hz) to get a reference level of the considered metrics. This is referred to as background in the remainder of the paper and the impact of the applied test signal is related to this level.

Most LED lamps and drivers show a reduction in the MD that can vary from 17% to 98% when subjected to SHs. The cause of this impact will be explained and illustrated in the following sections.

A. *Test #1 LED 02*

LED 02 consists of a full-bridge rectifier including a smoothing capacitor and a constant current regulator (CCR) [27]. The typical circuit diagram of a CCR LED driver is shown in Fig. 4.

SHs from 2 to 150 kHz have been applied on LED 02, as indicated in the testing method. Fig. 5 shows MD variation as a function of frequency and SH voltage. It should be noted that the calculations are performed with respect to background data,

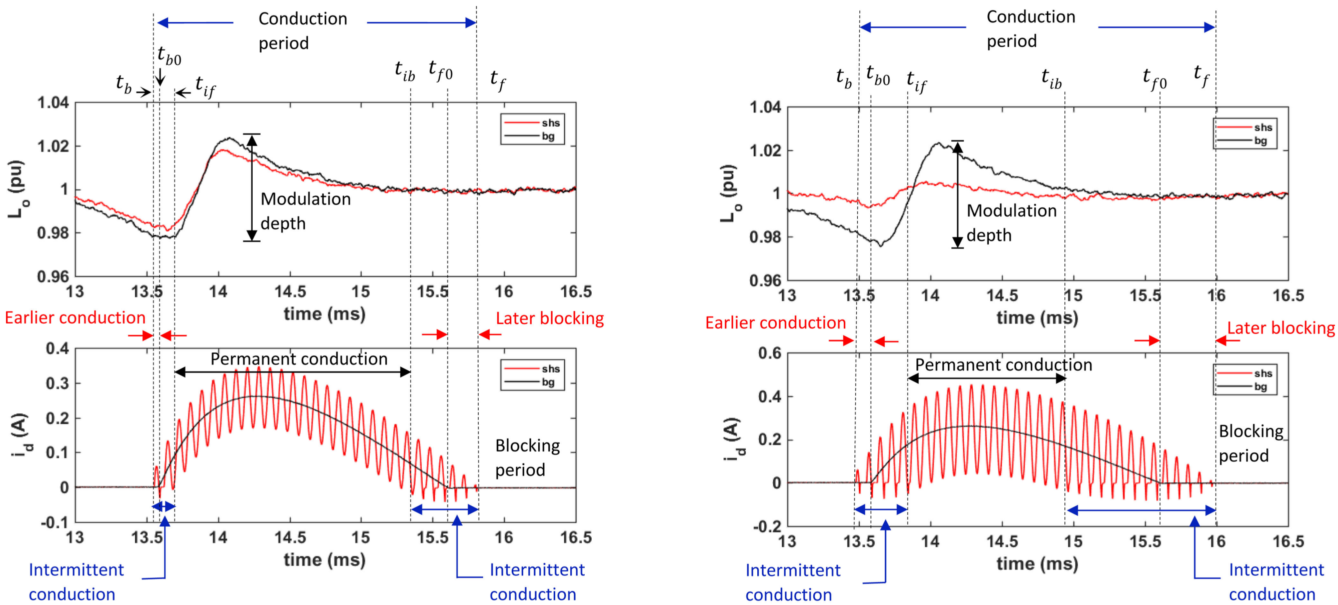

(a) (b)

Fig. 6. (a) Light intensity and input current of LED 02 at 3 V at 12.5 kHz. (b) Light intensity and input current of LED 02 at 7 V at 12.5 kHz.

where there is no injected SH. Per unit (p.u.) system is used, so that one-unity magnitude represents reference measurement. The presence of SHs results in a reduction of the MD. The higher the voltage, the more the MD is reduced. As the frequency of the SHs increases the impact is reduced, especially at higher voltage. The biggest impact is seen for voltage of 9 V at frequencies below 20 kHz and 12 V for frequencies below 40 kHz. A low MD, i.e., a more constant light intensity, is preferred; hence, the presence of SHs improves the performance of the lamp [19], [28].

In order to understand voltage-dependent factors behind the reduction in the MD, the signals have been analyzed in the time domain at two points, 3 V at 12.5 kHz [see Fig. 6(a)] and 7 V at 12.5 kHz [see Fig. 6(b)].

As shown in Fig. 6(a), the MD is reduced to 81% of the background level when the lamp is exposed to 3 V at 12.5 kHz. Two impacts are observed.

1) The diode starts conduction earlier (t_b) and blocks the current later (t_f) with respect to the background, therefore it consists of earlier conduction $(t_b - t_{b0})$ and later blocking $(t_{f0} - t_f)$ as given in Fig. 6.
2) A period of intermittent conduction occurs at the beginning $(t_b - t_{\text{if}})$ and at the end $(t_{ib} - t_f)$ of the current conduction period.

Definition of earlier conduction/later blocking and intermittent conduction provide the basis for the rest of the paper.

The same phenomenon takes place for 7 V at 12.5 kHz as seen in Fig. 6(b). In this case, the intermittent conduction is longer due to the increased SHs voltage. The result shows that the later blocking proceeds longer than the earlier conduction. This also leads to a change of the shape of the current waveform. This will be further discussed in Section IV. The middle of the current conduction period, the current fluctuates without becoming zero, is referred to as permanent conduction in the remainder of the paper. The MD drops to 27% under 7 V application, the impact is three times greater compared to the 3 V application for the same frequency.

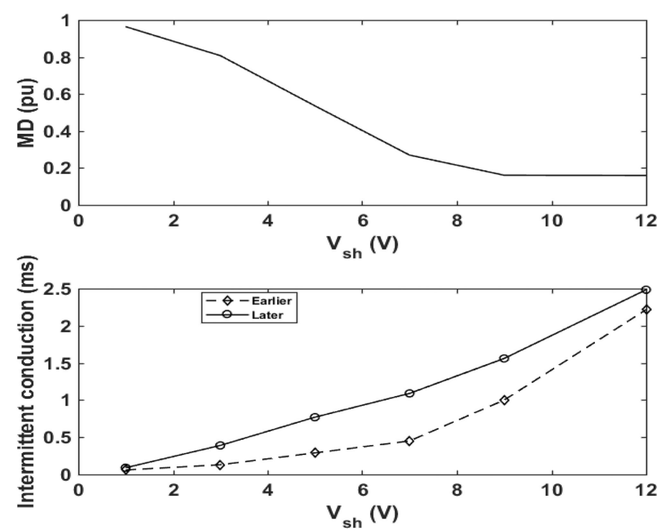

Fig. 7. Intermittent conduction and MD with respect supraharmonic voltage at 12.5 kHz supraharmonic voltages.

The analysis indicates that there is a link between the intermittent conduction and the MD of the light intensity variation. To calculate the intermittent conduction, a method that can locate the points where the intermittent conduction starts and stops is implemented. This is achieved by detecting any deviation, as the first and the last one found, from the zero current. The method is verified by manually locating the points of interest in the figures. The intermittent conduction and the MD are calculated and plotted with respect to the SH voltage as shown in Fig. 7. It shows that the intermittent conduction increases as the applied voltage increases. The analysis indicates that the earlier

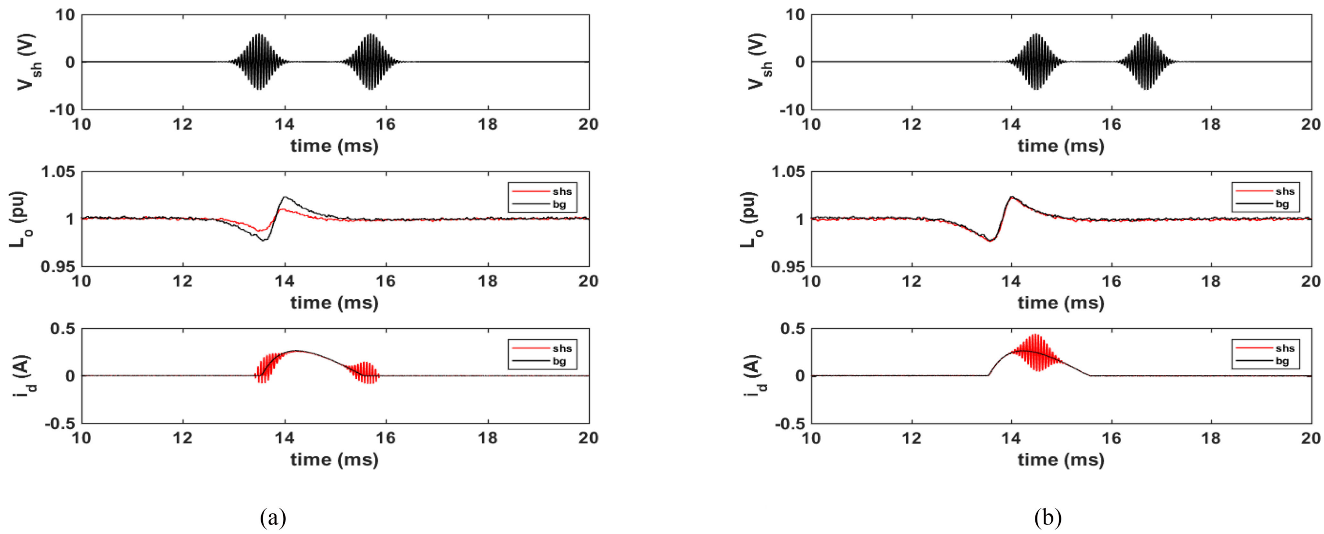

Fig. 8. Applied voltage profile, light intensity variations, and current drawn by the lamp (a) at the beginning and end of conduction period and (b) in the permanent conduction.

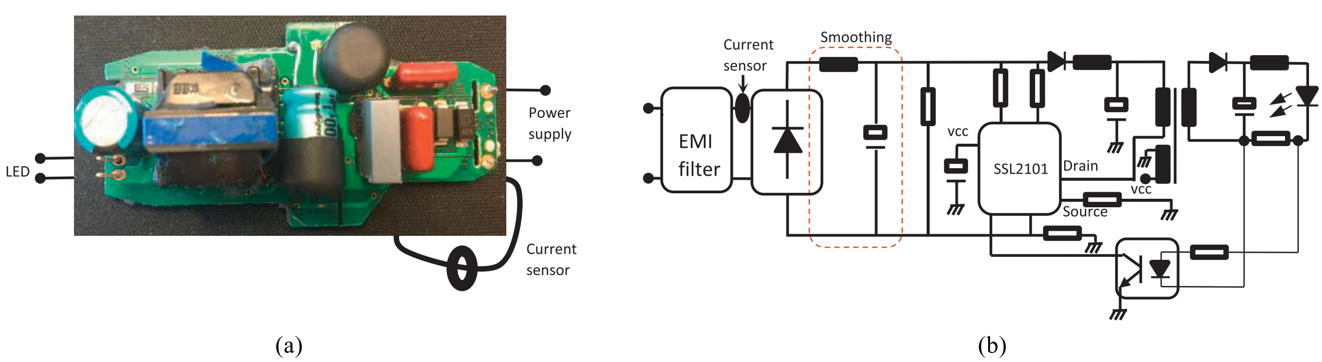

Fig. 9. (a) LED 14 internal circuit. (b) Electrical schematic for LED 14.

conduction/later blocking and the intermittent conduction contribute to the decrease in the MD.

An additional experiment has been performed in order to demonstrate the dependency of the position of SH distortion on the voltage waveform. Short-duration pulses of the SH profile have been applied at the beginning and at the end of the conduction period on LED 02 with 6 V_{peak} at 17 kHz. The pulse profile, the light intensity variations, and the current drawn by the lamp are given in Fig. 8(a). The MD drops to 50% with respect to background when the pulses appear at the beginning and at the end of the background conduction period.

In Fig. 8(b), the same profile is shifted 1 ms such that it shows up at the peak of the conduction period. The MD is not impacted in this case. It is also observed that there is no earlier conduction/later blocking and intermittent conduction.

The results show that the position of the SH on the supply voltage waveform impacts the MD. The reduction is observed where the SH appears at the beginning and end of the conduction period.

B. Test #2 LED 14

LED 14 consists of an electromagnetic interference (EMI) filter, a rectifier plus smoothing circuit, and a flyback dc–dc converter for controlling the LED voltage/current [29]. The current is acquired at the output of the EMI filter, just before the diode rectifier. The lamp has been disassembled for required modifications. Internal circuit of LED 14 and schematic are presented in Fig. 9.

Fig. 10(a) shows the MD during frequency sweeping for different SH voltage. The MD drops to 85% for 12 V, particularly for frequencies below 15 kHz. The reduction is present even for lower voltage. For instance, the SH voltage of 3 V leads to a reduction of more than 4% for frequencies below 20 kHz.

Increasing the SH voltage reduces the MD but increases the average light intensity as shown in Fig. 10(b). There is a dramatic change around 32 kHz in both the average light intensity and the MD. This will be discussed in Section IV-C.

Fig. 11 shows the same relation between the MD and the intermittent conduction as in LED 02. Increasing the SH voltage leads to longer intermittent conduction and the longer intermittent contribute to the reduction in MD.

C. Test #3 LV5011MD Evaluation Board

LV5011MD is a non-isolated buck–boost converter that contains an EMI filter as shown in Fig. 12 [30]. It is used for

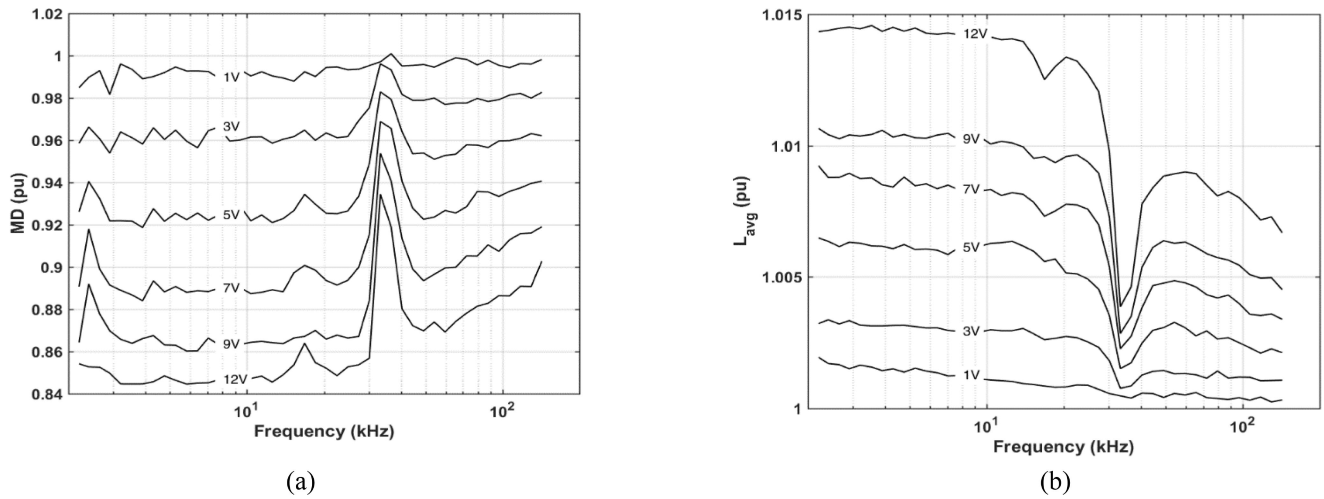

Fig. 10. (a) LED 14 MD as a function of frequency for various supraharmonic voltage. (b) LED 14 average light intensity for various supraharmonic voltage.

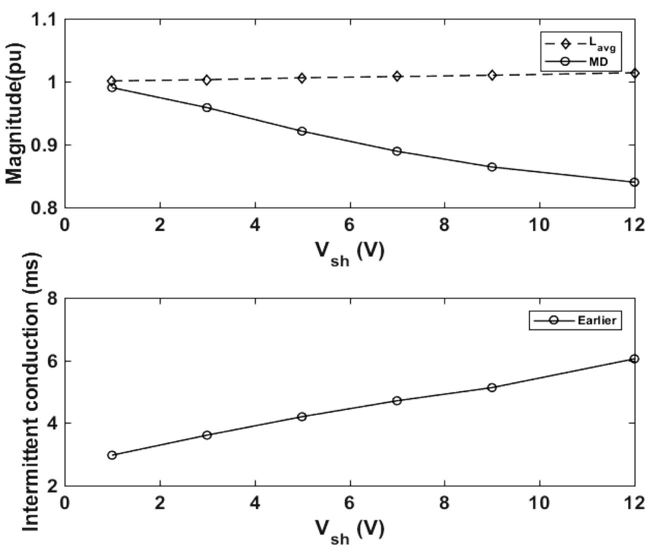

Fig. 11. Intermittent conduction and MD/average light intensity with respect to supraharmonic voltage at 12.5 kHz for LED 14.

residential and commercial LED lighting applications with dimming function.

The MD and the average light intensity are given in Fig. 13. The evaluation board exhibits less sensitivity under SHs but the impact follows the same trend as in the previous tests. In Fig. 13, the MD is reduced to 96.5% at 12 V and 10.3 kHz. At the same point, the average light intensity increases by 0.85% with respect to the background average light intensity.

The relationship between MD and the intermittent conduction is demonstrated in Fig. 14. The same phenomena as described for LED 02 and 14 can be observed in the evaluation board LV5011MD, too. Increasing the intermittent conduction leads to lower MD as well as an increase in the average light intensity.

When the SH frequency is higher, the diode starts drawing reverse-recovery current in the forward bias region. Fig. 15 illustrates how the diode conducts at two different frequencies. In Fig. 15(a), the diode reverse-recovery current is limited at 10.3 kHz compared to 142 kHz case given in Fig. 15(b). For a frequency of 142 kHz, the diode reverse-recovery current is much higher, as indicated in Fig. 15(b). The impact of the intermittent conduction on the MD is compensated by the reverse conduction in the forward bias region. We will further investigate this point in Section IV.

D. Summary of Observation

In summary, the following three phenomena can impact the MD/average light intensity:

1) The earlier conduction/later blocking;
2) The intermittent conduction;
3) The reverse-recovery current of the diodes.

The first two exhibit mainly SH voltage dependency and the latter mainly a frequency dependency.

IV. Development of AC–DC LED Driver Model Exposed To SHs

Each of the three mechanisms mentioned in Section III-D has been analyzed individually in terms of circuit theory in order to constitute a proper model and a qualitative explanation of the mechanism.

A. Earlier Conduction/Later Blocking

The two states of an ac–dc rectifier circuit are shown in Fig. 16. The relation between the supply voltage $v_s(t)$ and the dc-link voltage $v_d(t)$ defines the duration of the conduction period.

When the SH voltage is superimposed on the supply voltage, the input voltage to the diode rectifier $e_o(v_s, v_{\mathrm{sh}})$ becomes

$$e_o(t) = \sqrt{2}V_s \sin \omega t + \sqrt{2}V_{\mathrm{sh}} \sin\left(\frac{f_{\mathrm{sh}}\omega t}{f_s}\right) \tag{2}$$

where f_{sh} and f_s are the SH frequency and the supply frequency, respectively. Also, ω represents the angular frequency of the supply voltage, while V_s and V_{sh} are showing the rms value of supply voltage and SH voltage, respectively.

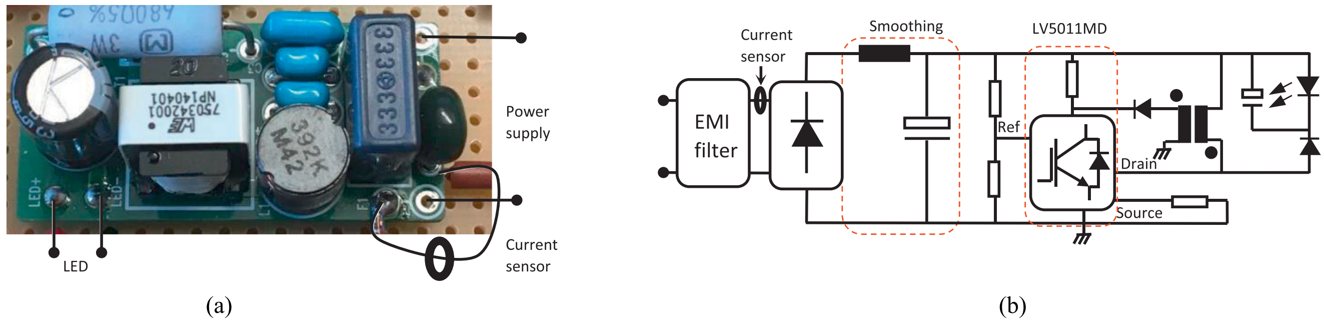

Fig. 12. (a) LV5011MD evaluation board. (b) Circuit configuration of the board.

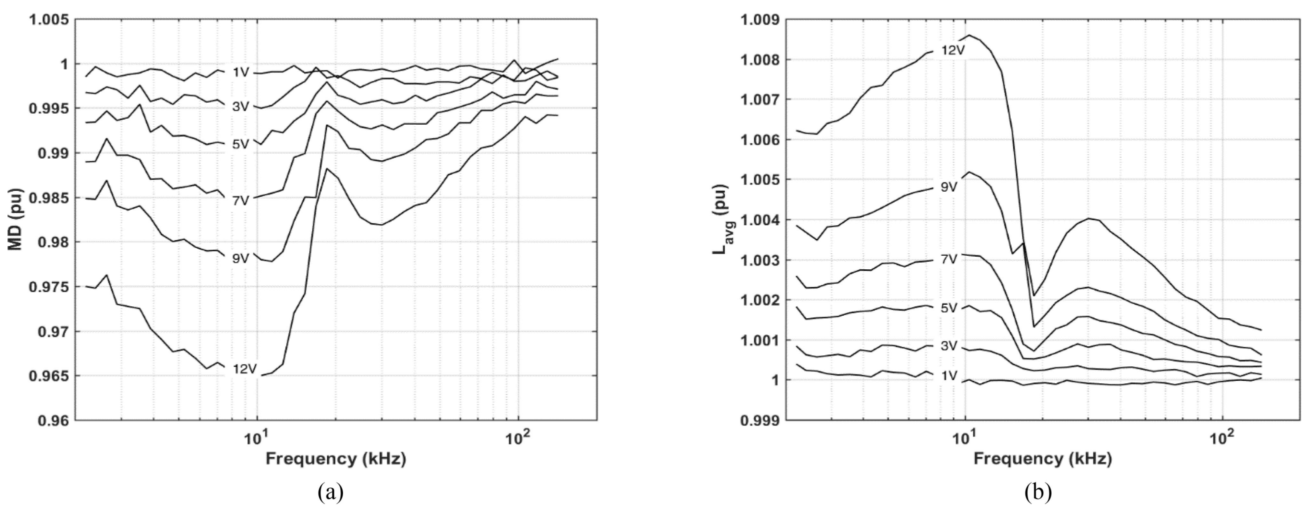

Fig. 13. (a) LV5011MD MD as a function of frequency for various supraharmonic voltages. (b) LV5011MD average light intensity as a function of frequency for various supraharmonic voltages.

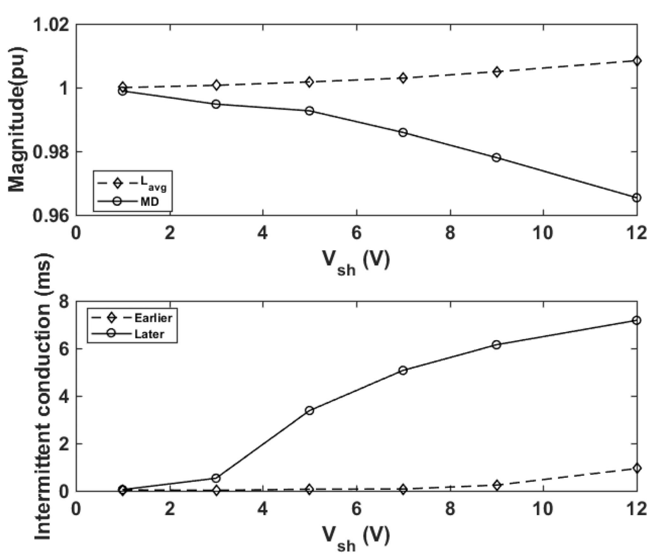

Fig. 14. Intermittent conduction and MD/average light intensity with respect to supraharmonic voltage at 12.5 kHz.

Conduction of the diode starts when the condition given in (3) is satisfied for the first time

$$e_o(t) > v_d(t) + 0.7 \text{ V}. \tag{3}$$

At the beginning of the conduction period, SH voltage oscillation adds to $e_o(t)$ causing the conduction to start earlier compared to the background conduction period. At the end of the conduction period, conduction stops at a current zero crossing, but restarts once (3) becomes valid again. This period of the intermittent conduction stops when (3) remains invalid during a complete SH period. The process (3) continuous until (3) is violated; very soon after the first violation, intermittent conduction appears, because of the SH oscillations in the current. The same phenomenon occurs at both sides of the conduction period; however, the later blocking takes longer due to the decrease in the supply voltage and dc-link voltage.

When the length of the conduction period increases, the load/capacitor is fed by the grid longer, which results in higher charging energy transfer and the dc-link voltage of the rectifier $v_d(t)$ increases. This increase causes the reduction of the rectifier dc-link voltage ripple and so MD. The impact of this on light intensity is visible in Fig. 6 for two different SH voltages.

The calculation of the time (t_b), when the diode start conduction under SHs, is partly possible if the voltage $v_d(t_f)$, when the diode stops conduction, is known. The time domain solution of $v_d(t)$ during the blocking period is expressed as follows:

$$v_d(t) = v_d(t_f)\, e^{-(t-t_f)/(C_d R_e)} \tag{4}$$

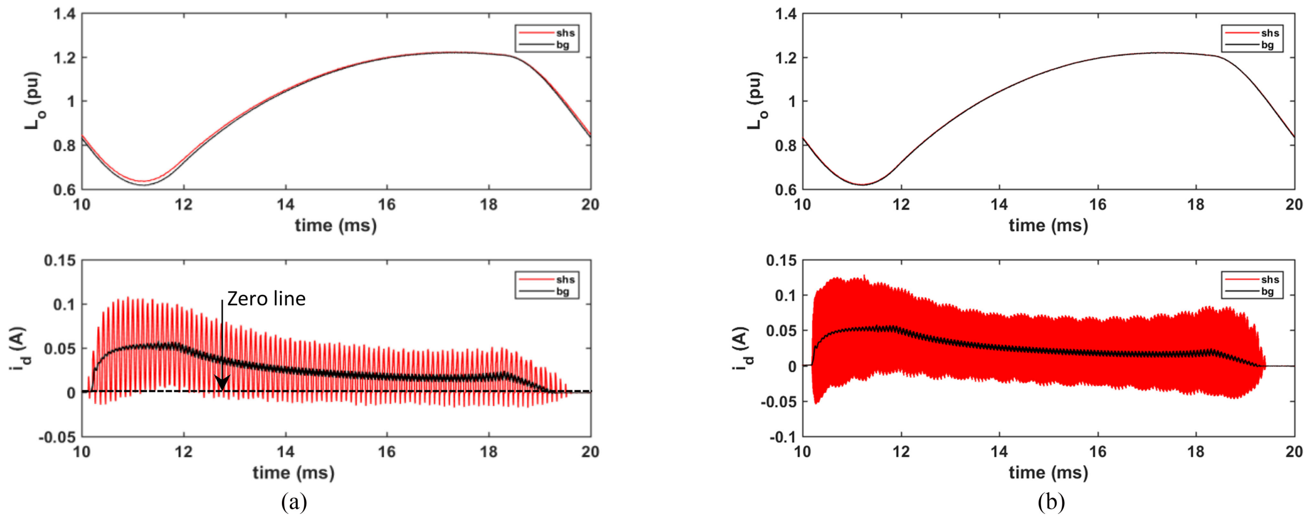

Fig. 15. Time domain signals for two different frequency. (a) Light intensity and input current of LV5011MD at 12 V and 10.3 kHz. (b) Light intensity and input current of LV5011MD at 12 V and 142 kHz.

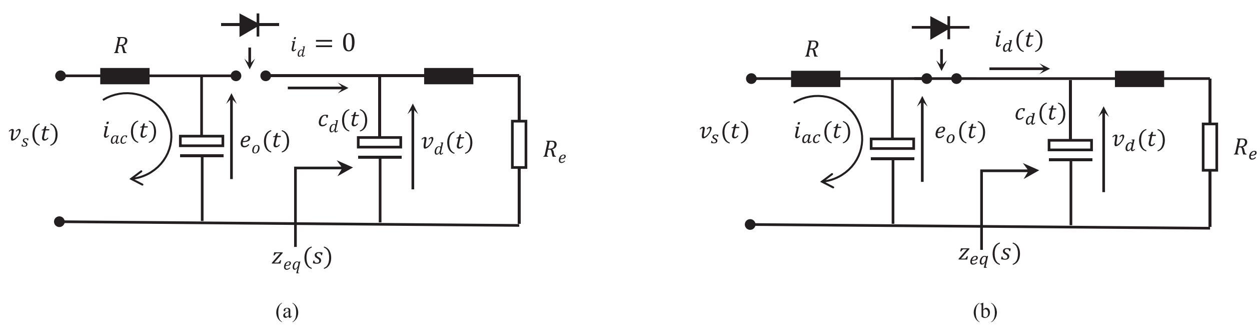

Fig. 16. Simplified equivalent circuit of an LED driver during (a) blocking and (b) conduction period.

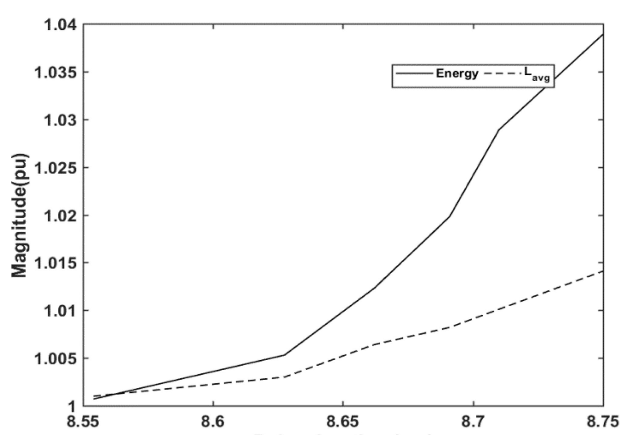

Fig. 17. Relation between half-cycle conduction period due to intermittent conduction and the charging energy/average light intensity for LED 14 at 12.5 kHz.

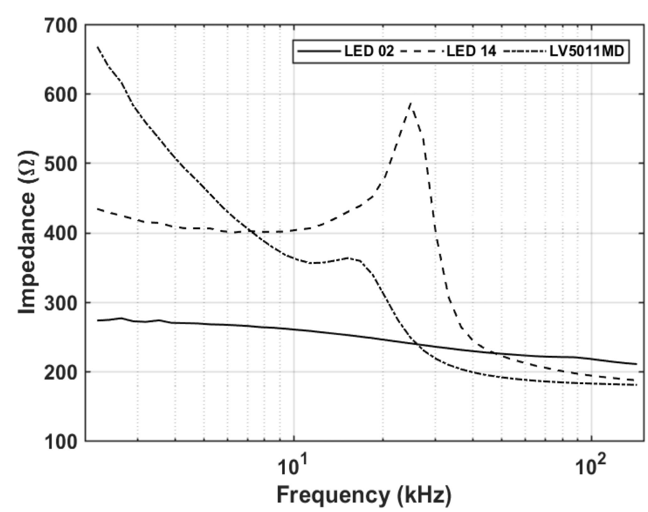

Fig. 18. Impedance characteristic of LED lamps at 9 V supraharmonic application.

where C_d is the dc-link capacitor and R_e is the dc-link load. At start of time (t_b), the following equation must be satisfied:

$$v_d\left(t_f\right) e^{-(t_b - t_f)/(C_d R_e)} = e_o\left(t_b\right). \tag{5}$$

The increased conduction period will also, generally, result in an increase in average light intensity. The impact is however not as easy to quantify and depends, among others, on dc-link voltage. This increase can, under certain assumptions, be explained as follows.

In Fig. 16, where $i_d(t)$ is the dc current and $i_{ac}(t)$ is the ac current, the charge that enters at AC side is, in steady state and averaged over a cycle, the same as the charge that leaves

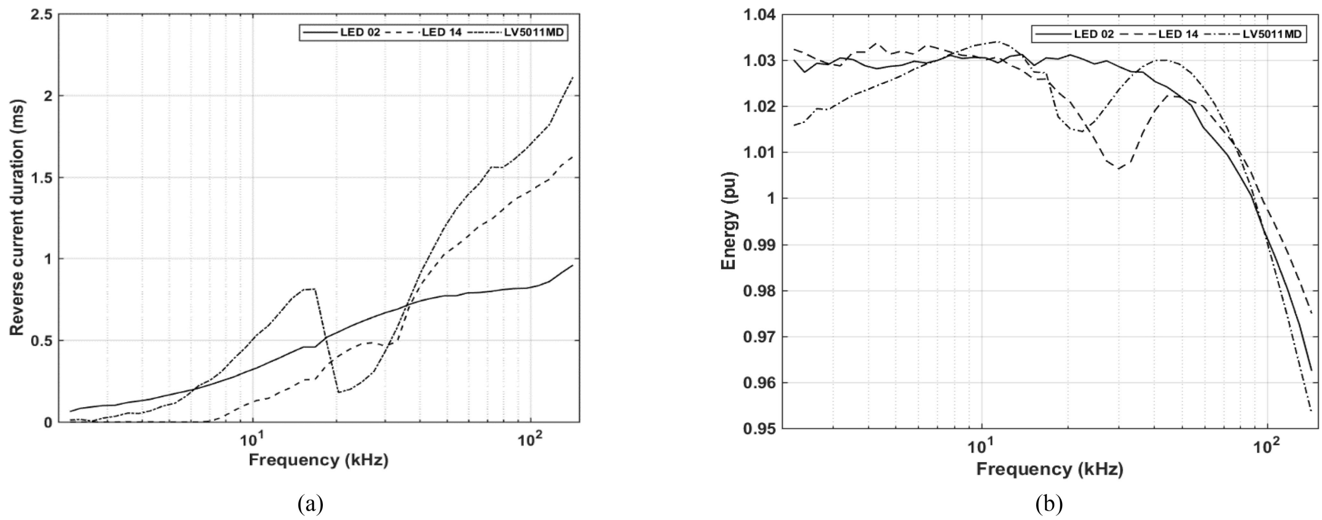

Fig. 19. (a) Reverse current duration with respect to frequency under 9 V. (b) Charging energy over a cycle at 9 V.

to the dc-link load. The intermittent conduction due to the SHs means that the charge that enters the ac side is outside of the background current conduction period $(t_{b0} - t_{f0})$. Assuming this extra charge is equal to $Q_{\rm sh}$ gives

$$Q_{\rm sh} + \int_0^{2\pi/\omega} |i_{\rm ac}(t)|\, dt = \int_0^{2\pi/\omega} i_d(t)\, dt \tag{6}$$

where $i_{\rm ac}(t)$ is the current at ac side in conduction and can be determined as follows:

$$i_{\rm ac}(t) = \frac{|e_o(t)| - V_d}{R} \tag{7}$$

where R is the supply resistance. If it is assumed that the dc current is constant and calculated by using load power P_e and dc-link voltage, we get (8) after dividing supply frequency cycle into four parts [31]

$$Q_{\rm sh} + \int_{t_1}^{\left(\frac{\pi}{2\omega} - t_1\right)} \frac{\sqrt{2}e_o \sin(\omega t)}{R} dt = \frac{1}{2\pi} \frac{P_e}{V_d}. \tag{8}$$

After performing the integration, it results in

$$V_d\sqrt{1 - V_d^2} - V_d^2\left[\frac{1}{2}\pi - \arcsin(V_d)\right] = \frac{1}{2}\pi\ P_e - V_d\omega Q_{\rm sh}. \tag{9}$$

The left-hand side expression is the same as in the no-SHs case [31], the impact of the additional conduction is, in the equation, the same as reduction in dc-link load P_e. As shown in Fig. 17, an additional conduction results in an increase in dc-link voltage, and so in average light intensity. The correlation between the half-cycle conduction period, charging energy, and average light intensity is given in Fig. 17 for LED 14. The different points in the curves were obtained by, at the same frequency of 12.5 kHz, changing the SH voltage.

B. Intermittent Conduction

Once the diode starts conducting, the system is linear. Depending on the SH equivalent impedance of the circuit, the SH current could be high enough to change the polarity of the current which results in the blocking of the current due to diodes. The blocking is continuous until the SHs oscillation is back to the right conduction region of the diode. If the impedance is lower, the SH current becomes higher. Higher current results in a longer intermittent conduction.

The measurement of the equivalent impedance as a function of frequency is shown in Fig. 18 for the three lamps. The impedance measurement method is defined and explained in [32].

The impedance characteristic defines how the large currents are drawn at the relevant SH. The larger the SH current, the longer the intermittent conduction, which results in more reduction in the MD. The correlation between the MD and the impedance characteristic is rather weak when the frequency is higher, particularly above 20 kHz, due to the diode reverse-recovery current impact.

C. Diode Reverse-Recovery Current

It has been observed that when the SH frequency increases, the current can cross to the reverse polarity zone where the diode is supposed to block it. The difference for two different frequencies is seen in Fig. 15(a) and (b), where LV5011MD is subjected to 10.3 and 142 kHz, respectively.

The reverse current duration as a function of frequency has been calculated within the half-cycle period for the three lamps as shown in Fig. 19(a). In addition, the charging energy over one cycle of the supply voltage is illustrated in Fig. 19(b). The charging energy drops while the diode reverse current duration increases, particularly above 50 kHz.

With increasing SH frequency, the duration of the reverse recovery increases. This reduces the charging energy over one cycle. It leads to an increase in the MD as shown in Figs. 5, 10(a), and 13(a), particularly above 50 kHz. The charging energy drops at 32 kHz for LED 14. It results in decreasing average light intensity and increasing MD as shown in Fig. 10. It verifies the link between the charging energy and average light intensity given in (9) as drop in the charging energy leads to decreasing

TABLE I
THREE PHENOMENA AND THEIR IMPACT ON LIGHT

Phenomenon	Dependency	Impact on light	
		MD	L_{avg}
Earlier conduction/ later blocking	Voltage and position of disturbance	decreased	increased
Intermittent conduction	Impedance and position of disturbance	decreased	increased
Reverse- recovery current of the diode	Frequency of disturbance	increased	decreased

average light intensity and increasing MD. The reason behind the drop in charging energy at 32 kHz is not fully understood. It corresponds to conduction period that changes the charging energy depending on the intermittent conduction. It should also be noted that the MD increases toward the background level due to reversing impact. The diode reverse-recovery current dominates to variation in the MD above 50 kHz.

V. Discussion and Conclusion

In this study, the impact of SHs on light intensity variations for LED lamps has been investigated. A test profile has been applied to the lamps and light intensity variations have been analyzed.

Three phenomena that can impact the MD have been observed from the experiments.

1) Earlier conduction/later blocking caused by SH voltage.
2) Intermittent conduction.
3) Reverse-recovery current of the diodes at higher frequencies.

The three phenomena, their dependency, and impact are summarized in Table I.

The combined impact of the earlier conduction/later blocking and intermittent conduction leads to an increase in the average light intensity and a reduction in the MD. There is a strong correlation between the increase in the conduction period, the charging energy, and the average light intensity.

The diode starts reverse-recovery current conduction at higher frequency that decreases the total charging energy, so it results in decreasing average light intensity as shown in Figs. 10 and 13. The reduction in the transferred energy is notable above 50 kHz as shown in Fig. 19(b), but still effective above 16 kHz depending on the other variables.

The reduction in the MD is an improvement in terms of light quality. The issue of earlier conduction and later blocking could show up in the drivers, which have shorter conduction periods. If the rectifier's power factor is corrected as unity or above 95%, hence the nonlinearities are overcome, no earlier conduction or later blocking is possible, so the impact can be reduced by using active power factor correction circuit, yet it cannot be guaranteed due to possible other type of interactions between the SHs and the lamp's driver.

The test profile has been applied based on the IEC 61000-4-19 CW signal that exist within the entire cycle of the supply voltage. It is shown that the impact of the SHs on the MD and average light intensity occurs when the distortion appears around the time the device starts or ends its current draw. A distortion present at these moments leads to earlier conduction/later blocking and intermittent conduction. Any distortion that appears in the conduction time has no or limited effect, unless the current is of high enough magnitude to cause reverse conduction of the diodes. This also shows the importance of the position of the SH distortion in the background waveform, known as "point on wave." The standard testing method describes no information how to test the impact of "point on wave" for equipment. This issue shall be taken into account by the standard committees.

This study is limited to the application of SHs at one frequency at a time. However, the emission in the grid consists of the combination of different SH frequencies, which could lead to more complex impacts. Descriptive models presented in this paper can also be used for better understanding of combined effect of SHs at different frequencies. Also, the impact of actual signals, measured in the grid, need to be investigated in future studies.

Since the impact of SHs on the light intensity originates from the dc-link voltage ripple of the rectifier, the descriptions concluded in this paper are valid for ac–dc rectifiers, in general. When a rectifier is exposed to SHs, the voltage ripple decreases, and the average dc-link voltage increases. This is, for most applications, an improvement in the performance of the rectifier. The shape of the current waveform changes due to different durations of earlier conduction and later blocking. It shows up as a shift in the current, which affects the reactive power flow in the rectifier.

Appendix

See Table II.

TABLE II
AC–DC LED DRIVER BOARD AND LAMPS

Symbol	Power(W)	PF	DC Voltage	f_{sw}
LED 02	11	0.55	14	NA
LED 14	8	0.65	40	100 kHz
LV5011MD	5	0.74	48	70 kHz

References

[1] J. Meyer *et al.*, "Future work on harmonics - Some expert opinions Part II - Supraharmonics, standards and measurements," in *Proc. Int. Conf. Harmon. Qual. Power*, Bucharest, Romania, Jun. 2014, pp. 909–913.

[2] S. K. Rönnberg, M. H. J. Bollen, and M. Wahlberg, "Interaction between narrowband power-line communication and end-user equipment," *IEEE Trans. Power Del.*, vol. 26, no. 3, pp. 2034–2039, Jul. 2011.

[3] S. K. Rönnberg *et al.*, "On waveform distortion in the frequency range of 2 kHz–150 kHz—Review and research challenges," *Elect. Power Syst. Res.*, vol. 150, pp. 1–10, Sep. 2017.

[4] P. Kotsampopoulos *et al.*, "EMC Issues in the interaction between smart meters and power-electronic interfaces," *IEEE Trans. Power Del.*, vol. 32, no. 2, pp. 822–831, Apr. 2017.

[5] NSAI, Dublin, Ireland, "Study report on electromagnetic interference between electrical equipment/systems in the frequency range below 150 kHz," NSAI Standards, Irish Standard Recommendation, S.R. CLC/TR 50627, 2013.

[6] S. Sakar, S. Rönnberg, and M. H. J. Bollen, “Immunity test of LED lamps based on IEC 61000-4-19 and unexpected consequence,” in *Proc. 18th Int. Conf. Harmonics Quality Power*, Ljubljana, Slovenia, May 2018, pp. 13–16.

[7] Electromagnetic Compatibility (EMC)-Part 4-19: Testing and Measurement Techniques – Test for Immunity to Conducted, Differential Mode Disturbances in the Frequency Range 2 kHz to 150 kHz at A.C. Power Ports, IEC 61000-4-19, 2012.

[8] S. Rönnberg, “Emission and interaction from domestic installations in the low voltage electricity network, up to 150 kHz, ” Ph.D. dissertation, Dept. Eng. Sci. Math, Luleå Univ. Technol., Skellefteå, Sweden, 2013.

[9] G. K. J. Kirchhoff, “Deficits and uncertainties in photovoltaic 902 inverter test procedures,” in *Proc. 24th Eur. PV Sol. Conf. Exhib.*, Hamburg, Germany, Sep. 2009, pp. 1–4.

[10] Y. Guo, S. Li, A. T. L. Lee, S.-C. Tan, C. K. Lee, and S. Y. R. Hui, “Single-stage AC/DC single-inductor multiple-output LED drivers,” *Trans. Power Electron.*, vol. 31, no. 8, pp. 5837–5850, Aug. 2016.

[11] R. Lenk and C. Lenk, *Practical Lighting Design With LEDs*. Hoboken, NJ, USA: Wiley, 2011.

[12] P. Fang, Y.-F. Liu, P. C. Sen, “A flicker-free single-stage offline LED driver with high power factor,” *IEEE J. Emerg. Sel. Topics Power Electron.*, vol. 3, no. 3, pp. 654–665, Sep. 2015.

[13] Electromagnetic Compatibility (EMC)- TR 61547-1: Equipment for *General Lighting Purposes*- EMC *Immunity Requirements*- Part 1: *An Objective Light Flickermeter* and *Voltage Fluctuation Immunity Test Method*, IEC TR 61547-1, 2017.

[14] United States Department of Energy, Alexandria, VA, USA, “Caliper. retail lamps study 3.1: Dimming, flicker, and power quality characteristics of a LED A lamps,” Retail Lamp Study 3.1. Dec. 2014.

[15] A. Gil-de-Castro, S. K. Rönnberg, and M. H. J. Bollen, “Light intensity variation (flicker) and harmonic emission related to LED lamps,” *Elect. Power Syst. Res.*, vol. 146, pp. 107–114, May 2017.

[16] Electromagnetic Compatibility (EMC)- Part 4-15: Testing and *Measurement Techniques- Flickermeter- Functional* and *Design Specifications*, IEC 61000-4-15, 2010.

[17] B. Lehman, A. Wilkins, S. Berman, M. Poplawski, and N. Johnson Miller, “Proposing measures of flicker in the low frequencies for lighting applications,” in *Proc. IEEE Energy Convers. Congr. Expo.,* Phoenix, AZ, USA, 2011, pp. 2865–2872.

[18] *IEEE Recommended Practices for Modulating Current in High-Brightness LEDs for Mitigating Health Risks to Viewers*, IEEE 1789-2015, 2015.

[19] Y. Ko, H. S. Cho, S. S. Lee, S. B. Shin, Y. Song, and S. G. Lee, “A compact flicker-free transformer-less LED driver with an enhanced power factor for omnidirectional multichannel smart bulb applications,” *IEEE Trans. Power Electron.*, vol. 31, no. 8, pp. 5851–5862, Aug. 2016.

[20] H. C. Kim, M. C. Choi, S. Kim, and D. K. Jeong, “An AC-DC LED driver with a two-parallel inverted buck topology for reducing the light flicker in lighting applications to low-risk levels,” *IEEE Trans. Power Electron.*, vol. 32, no. 5, pp. 3879–3891, May 2016.

[21] S. K. Rönnberg, M. Wahlberg, E. O. A. Larsson, M. H. J. Bollen, and C. M. Lundmark, “Interaction between equipment and power line communication: 9–95 kHz,” in *Proc. IEEE Bucharest PowerTech*, Bucharest, Romania, 2009, pp. 1–5.

[22] S. Rönnberg, M. Wahlberg, M. Bollen, and A. Larsson, “Measurements of interaction between equipment in the frequency range 9 to 95 kHz,” in *Proc. 20th Int. Conf. Exhib. Elect. Distrib.*, Prague, Czech Republic, Jun. 2009, pp. 8–11.

[23] G. Singh, “Characterizing light output variations from solid state lighting due to high frequency electromagnetic interference,” Ph.D. dissertation, Dept. Elect. Eng, Graduate School Clemson Univ., Clemson, SC, USA, May 2016.

[24] D. Agudelo-Martinez, F. Rios, and A. Pavas, “Interaction of some low power LED lamps within 2–150 kHz (supraharmonics),” in *Proc. 18th Int. Conf. Harmonics Quality Power*, Ljubljana, Slovenia, May 2018, pp. 13–16.

[25] G. Singh, E. R. Collins, E. O. A. Larsson, and M. H. J. Bollen, “Impact of high frequency conducted voltage disturbances on led driver circuits,” in *Proc. IEEE Power Energy Soc. Gen. Meeting*, Chicago, IL, USA, Jul. 2017, pp. 1–5.

[26] A. Wilkins, J. Veitch, and B. Lehman, “LED lighting flicker and potential health concerns: IEEE standard PAR1789 update,” in *Proc. IEEE Energy Convers. Congr. Expo.*, Atlanta, GA, USA, Sep. 2010, pp. 171–178.

[27] Duty Semiconductor, Datasheet, DU1502, pp. 1–8, Apr. 2015.

[28] P. Fang and Y. F. Liu, “Energy channeling LED driver technology to achieve flicker-free operation with true single stage power factor correction,” *IEEE Trans. Power Electron.*, vol. 32, no. 5, pp. 3892–3907, May 2017.

[29] NXP Semiconductors, Eindhoven, The Netherlands, “AN10829 SSL2101 dimmable high efficiency flyback design,” Application note, Jun. 2011.

[30] On Semiconductor, Phoenix, AZ, USA, “LV5011MD-GU10-230VEVM03, the buck-boost converter for phase cut dimming with high power factor,” Application note, Jul. 2014.

[31] M. H. J. Bollen and I. Y. H. Gu, *Signal Processing of Power Quality Disturbance*. Hoboken, NJ, USA: Wiley, Aug. 2006.

[32] T. Busatto, V. Ravindran, A. Larsson, and M. H. J. Bollen, “Estimation of the consumer electronics capacitance for harmonic resonance studies by a non-invasive measurement method,” in *Proc. 18th Int. Conf. Harmonics Quality Power*, Ljubljana, Slovenia, May 2018, pp. 13–16.

Selcuk Sakar (S’14) received the B.Sc. and M.Sc. degrees from the Graduate School of Natural and Applied Sciences, Gazi University, Ankara, Turkey, in 2010 and 2012, respectively. He is currently working toward the Ph.D. degree in electrical power engineering at the Luleå University of Technology, Skellefteå, Sweden.

His current research interests include power quality, ac–dc LED drivers exposed to voltage disturbances, and lighting and light flicker.

Sarah Rönnberg (SM’18) received the Ph.D. degree in electrical power engineering from the Luleå University of Technology, Skellefteå, Sweden, in 2013.

She is currently an Associate Professor with the Department of Engineering Sciences and Mathematics, Luleå University of Technology. Her research interests include supraharmonics, power system harmonics, and power quality in general.

Math Bollen (M’93–SM’96–F’05) received the M.Sc. and Ph.D. degrees from the Eindhoven University of Technology, Eindhoven, The Netherlands, in 1985 and 1989, respectively.

He is currently a Professor in electric power engineering with the Luleå University of Technology, Skellefteå, Sweden. Earlier he has, among others, been a Lecturer with the University of Manchester Institute of Science and Technology (UMIST), Manchester, U.K., a Professor in electric power systems with Chalmers University of Technology, Gothenburg, Sweden, an R&D Manager and Technical Manager power quality and distributed generation with STRI AB, Gothenburg, Sweden, and Technical Expert at the Energy Markets Inspectorate, Eskilstuna, Sweden.

He has authored and coauthored a few hundred papers including a number of fundamental papers on voltage dip analysis, two textbooks on power quality, “*Understanding Power Quality Problems*” and “*Signal Processing of Power Quality Disturbances*,” and two textbooks on the future power system: “*Integration of Distributed Generation in the Power System*” and “*The Smart Grid - Adapting the Power System to New Challenges*.” He has defined voltage dips as a research subject, has spread the use of the term “hosting capacity,” and has contributed to defining supraharmonics as a research area.

Dr. Bollen was the recipient of the CIGRE Study Committee Award.